

doi:10.15199/48.2024.05.33

Analysis and Design of Superstrate for Gain Enhancement of Meta-Surface Antenna

Abstract. This article is focusing on a technical design of superstrate layer using 3x3 unit cells to enhance the antenna gain, operating at the center frequency of 2.50 GHz. In fabrication of the proposed antenna, a microstrip antenna is fed by a 50Ω-SMA 3.50 mm connector, and the superstrate is designed using 9 octagon ring-shaped unit cells, which are integrated to form a meta-surface antenna (MS antenna). A prototype antenna is manufactured on an FR4 substrate material with a relative permittivity (ϵ_r) of 4.3 and a height of 1.6 mm. The prototype antenna is great matched to achieve $|S_{11}|$ of -31.55 dB, exhibits a gain enhancement of >2.0 dBi and achieves a maximum gain of >6.0 dBi. Additionally, the proposed design has been fabricated to validate $|S_{11}|$, gain, and radiation patterns as comparing with the simulated results that will be presented. Evidently, the simulated results reasonably align with the experimental findings.

Streszczenie. W artykule skupiono się na projekcie technicznym warstwy superstratnej wykorzystującej ogniwa elementarne 3x3 w celu zwiększenia zysku anteny, pracującej na częstotliwości środkowej 2,50 GHz. Podczas produkcji proponowanej anteny antena mikropaskowa jest zasilana przez złącze 50 Ω-SMA 3,50 mm, a superstrata została zaprojektowana przy użyciu 9 ośmiokątnych ogniw elementarnych w kształcie pierścienia, które są zintegrowane, tworząc antenę metapowierzchniową (antena MS). Prototypowa antena jest produkowana na podłożu FR4 o przenikalności względnej (ϵ_r) wynoszącej 4,3 i wysokości 1,6 mm. Prototypowa antena jest doskonale dopasowana do osiągnięcia $|S_{11}|$ -31,55 dB, wykazuje wzmocnienie wzmocnienia >2,0 dBi i osiąga maksymalne wzmocnienie >6,0 dBi. Ponadto proponowany projekt został opracowany w celu sprawdzenia $|S_{11}|$, wzmocnienia i wzorców promieniowania w porównaniu z symulowanymi wynikami, które zostaną zaprezentowane. Najwyraźniej symulowane wyniki są w rozsądny sposób zgodne z wynikami eksperymentów. (**Analiza i projektowanie superstratu w celu poprawy wzmocnienia Antena metapowierzchniowa**)

Keywords: Gain enhancement, Microstrip antenna, Meta-surface, Superstrate.

Słowa kluczowe: Wzmocnienie wzmocnienia, antena mikropaskowa, metapowierzchnia, superstrate.

Introduction

Wireless communication systems are continuously developing on the advance technology of antennas with the characteristic requirements including wide bandwidth, compact size, low profile, high gain radiation, easy integration, and cost-effectiveness. These properties will be helpfully employed to enhance communication distances, boost transmission data rates, and reduce the overall volume and size of the system. For these requirements, it can be possible by using a microstrip antenna that will become an essential component used in the modern wireless communication system. It can offer versatility and cost-effectiveness while delivering high-quality signals. The advantages of this antenna include low manufacturing costs, a lightweight design, directivity, and seamless integration with Monolithic Microwave Integrated Circuit (MMIC) designs [1-2]. In addition, this antenna is a planar antenna that is too sensitive with the effects of electromagnetic (EM) surface waves on the substrate. It can beneficially gain to forming the lobes, alter the radiation direction, upgrade overall the antenna performance, and high radiating gain [3].

Nowadays, researchers are interesting on a meta-surface (MS) technology that can be applicable to antenna design and be developing gain enhancement techniques [4]. There are many interested design techniques of microstrip antennas are related in this work. A metamaterial structure can be employed with the microstrip antenna design technique by adding the structure to improve the antenna gain of >3.00 dBi [5-6]. A superstrate material technique can be making an in-phase electric field on the top of the superstrate that was obtained gain of >8.00 dBi [7-11]. A shorting pins technique can be used to increase the effective electrical size of antenna [12]. In addition, it can control the current on radiating plate and ground plane is in the same direction resulting in superposition of radiation was achieved gain of <2.00 dBi. A metallic reflectors technique was popular in design with the reflector and adds to the main radiation and hence increase the gain

in the boresight direction with create in-phase radiation that was occurred gain of >8.00 dBi [13-14]. Also, the substrate removal technique by reducing the losses of the antenna in order to improve the antenna gain as more than 5.00 dBi [15]. From the above reviews, the superstrate material technique was interested and bring the concept to design and fabrication the antennas that will be presented in this paper. Several recent research has proposed the technical design of unit cell shapes on superstrate layer. In 2019, Kingsta R. M. et al. proposed the superstrate of 3x8 unit cells with the difference I-shaped and integrated array microstrip antenna with 9 radiating plate for obtained peak gain of 9.90 dBi at 5.90 GHz [16] and Aqeel H. N. et al. demonstrated the superstrate of 4x4 square-ring plate array and designed microstrip antenna with rectangular-shaped radiating plate whereas inserted U-slotted for generated radiation beam-steering and peak gain 5.70 dBi at 2.62 GHz [17]. In 2020, Diptiranjan S. et al. illustrated the superstrate of 5x5 unit cells with C and L-shaped were integrated a fractal-shaped slotted radiating plate antenna with shorting via into the ground plane were generated realized gain of 7.57 dBi at 10.44 GHz [18], Chandrashekar K. S. et al. depicted metal-ring superstrate and microstrip antenna with rectangular-shaped radiating plate for increased peak gain of >9.00 dBi at 9.70 GHz [19] and ,Avanish Y. et al. proposed superstrate with square-shaped unit cells and integrated MS horn antenna was achieved the maximum gain of 9.20 dBi at 2.45 GHz [20]. In 2021, Luiza L. et al. proposed the superstrate of 5x5 unit cells with the difference square-shaped and integrate microstrip antenna with designed square-shaped radiating inserted hexagonal-shaped slot can be generated radiation gain of >10.00 dBic (8.00-9.40 GHz) [21]. In 2022, Tamara Z. F. et al. proposed the superstrate of 4x4 unit cells are designed with a hybrid MS using square slit ring resonator (SSRR) unit cell for increased gain they found that U-shaped unit cell for split beam were integrated microstrip antenna and they were radiation gain enhancement of 6.74 dBi at 3.50 GHz [22] and in 2023, Anirban Ch. et al. presented a difference

rectangular metal-grids superstrate and integrated the fabry-perot cavity antenna (FPCA) for generated broadside gain of >11.50 dBi (11.50-17.40 GHz.) [23].

From above literature reviews, it can achieve a key for designing the superstrate layer of the proposed MS antenna. The superstrate layer was considered and analyzed the shape of unit cell resulting to the total transmission coefficient approaches or $|S_{11}|$ of 0 dB and phase of the reflection equal to -180° or 180° . Besides, the superstrate layer was designed and enhanced radiation gain for using in the modern wireless communication systems. In this article, we propose an analysis and design microstrip antenna integrated superstrate layer to enhance radiation gain. In the fabrication of the proposed antenna was the simple square-shaped plate of the microstrip antenna and superstrate layer was designed of 3×3 unit cells by an octagonal-shaped annular ring for increased gain of >6.50 dBi at the center frequency of 2.50 GHz. The antenna simulation is performed using the CST microwave studio software [24]. Also, the results will exhibit the significant improvements in the $|S_{11}|$, phase of reflection and radiation gain. This paper will be presented by separating in subsequent sections as follows: Section II covers the parametric investigation of the original antenna and the superstrate layer in the suggested design. Section III focuses on the results obtained from simulations and measurements, particularly in relation to $|S_{11}|$, gains, and radiation patterns. These simulations were performed using the CST microwave studio 2021 software. Finally, Section V offers concluding statements.

Parametric study

This section presents the design of the initial antenna state, the superstrate layer state, and the MS antenna state, including the presentation of experimental findings for the prototype antenna. The MS antenna is configured to operate at a center frequency of 2.50 GHz. The antenna is designed to construct as square-shaped structure (W_g) is 80.00 mm, height (h_d) of FR4 substrate ($\epsilon_r = 4.3$) is 1.60 mm and the copper layer has a thickness (t_g) is 35.00 μm . Additionally, the radiating plate is square with a width (w) of 28.00 mm. The radiating plate is fed by 50- Ω SMA 3.50 mm connector at the distance (d_p) from the center of radiating plate to the feeding point is 5.80 mm. The separation (S_a) from the superstrate layer to the microstrip antenna is 80.00 mm. The superstrate layer consists of a 3×3 array of unit cells, with each unit cell taking the form of an octagon ring shape unit cell. It is characterized by the radius (r_1) of octagonal-shaped plate, along with the inner radii (r_2) and outer radii (r_3) of the octagonal-shaped annular ring plate, which measure 7.00 mm, 9.00 mm, and 12.00 mm, respectively. All of described dimension details will be shown in Figure 1.

The microstrip antenna at stage#1, the initial antenna encompasses the square-shaped structure antenna (W_g) is 80.00 mm, height (h_d) of FR4 substrate material ($\epsilon_r = 4.3$) is 1.60 mm, the thickness of copper (t_g) is 35.00 μm and feeding point (d_p) is 5.80 mm. According to [1-3], the width of the square radiating plate at the center frequency of 2.50 GHz was determined as 36.8 mm. In Figure 2(a), the simulated $|S_{11}|$ is shown for varying widths (w) ranging from 19.20 mm to 36.80 mm, centered at a frequency of 2.50 GHz. The simulation indicated that a width (w) of 28.00 mm was optimal, resonating at the center frequency with $|S_{11}|$ of -17.45 dB. A width of 32.40 mm resonated at a frequency of 2.17 GHz with $|S_{11}|$ of -30.76 dB. A width of 23.60 mm resonated at a frequency of 2.96 GHz with $|S_{11}|$ of -10.90 dB. Widths of 19.20 mm and 36.80 mm

(matching the above calculation) resulted in impedance mismatches, respectively.

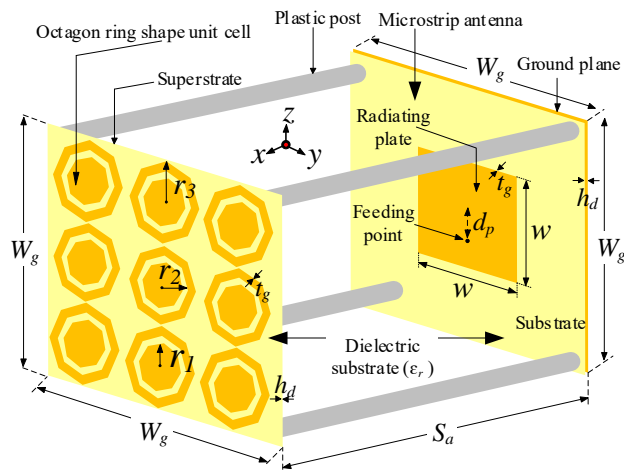


Fig. 1. The proposed structure MS antenna

The simulation results shown in Figure 2(b) shows the antenna gains for different values of width (w) at the center frequency of 2.50 GHz. The antenna gains are -14.40 dBi, -9.20 dBi, 4.39 dBi, -9.57 dBi, and -14.90 dBi for widths of 19.20 mm, 23.60 mm, 28.00 mm, 32.40 mm, and 36.80 mm, respectively. The maximum gains are 2.98 dBi, 4.39 dBi, and 4.16 dBi for widths of 32.40 mm, 28.00 mm, and 23.60 mm at the frequencies of 2.20 GHz, 2.50 GHz, and 2.96 GHz, respectively.

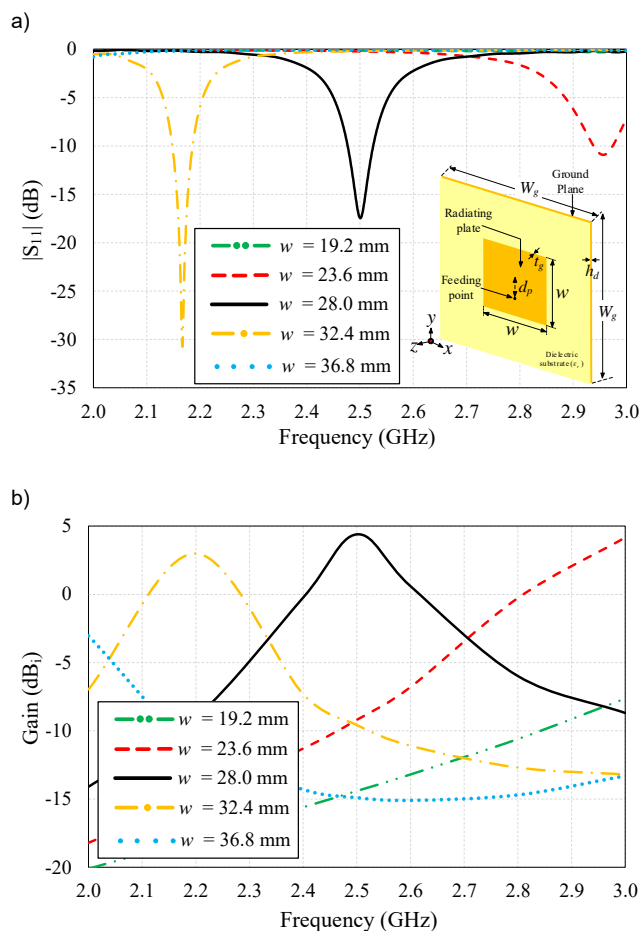


Fig. 2. The simulation results by varying width (w) of square radiating plate without superstrate (state#1): a) $|S_{11}|$ and b) gain.

In Stage #2, the superstrate layer is introduced. This stage focuses on making a superstrate of 3x3, which is applied to the octagon ring-shaped unit cell to enhance the radiation gain of the proposed MS antenna (Stage #3). As the waves travel through the superstrate layer, they align themselves parallel to free space, as enabling higher directivity. In state #2, the simulation is focused on analyzing and designing $|S_{11}|$, along with the phase of the reflection of the superstrate layer. This simulation demonstrates that the total transmission coefficient approaches 1 (i.e., 0 dB), or $|S_{11}|$ is close to 0 dB, with a reflection phase of 180° or -180° .

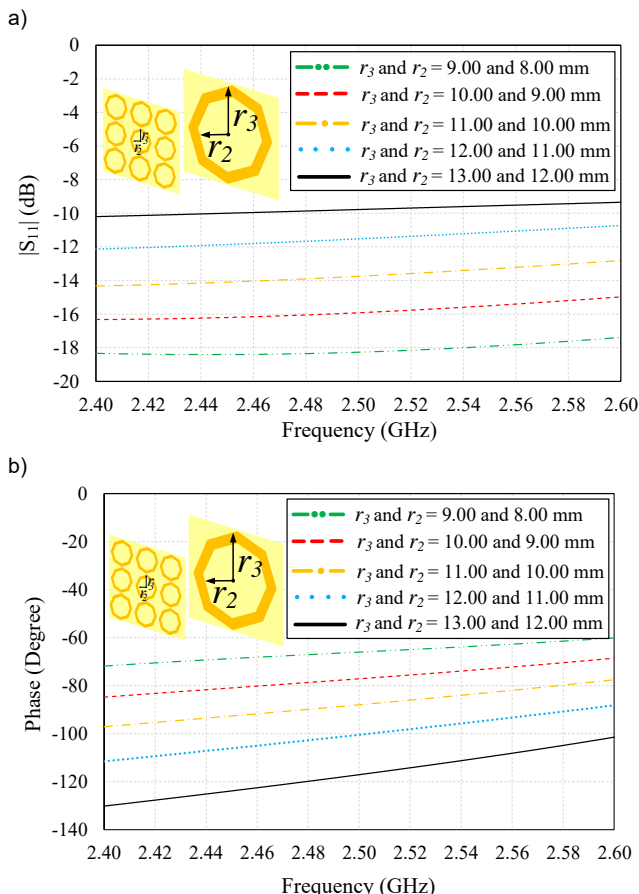


Fig. 3. The simulation results by varying pair inner radii (r_2) and outer radii (r_3) of octagonal-shaped annular ring plate (state#2): a) $|S_{11}|$ and b) phase of the reflection

The square-shaped structure of superstrate layer (W_g) is 80.00 mm, the height (h_d) of FR4 substrate ($\epsilon_r = 4.3$) is 1.60 mm and the thickness of the copper (t_g) is 35.00 μm . In this stage, a parametric study was conducted to observe the radius (r_1) of the octagonal-shaped plate, and also the inner radii (r_2) and outer radii (r_3) of the octagonal-shaped annular ring plate. The outer and inner radii (r_3 and r_2) of the pairs of octagonal-shaped annular ring plates are concurrently varied as follows: 9.00 and 8.00 mm; 10.00 and 9.00 mm; 10.00 and 9.00 mm; 11.00 and 10.00 mm; 12.00 and 11.00 mm; and 13.00 mm and 12.00 mm. The respective simulation results are illustrated in Figure 3. Specifically, Figure 3 (a) shows the simulated superstrate with octagonal-shaped annular ring plates arranged in a 3x3 configuration. However, it is important to note that the value of r_3 is constrained to not exceed 13.00 mm in order to prevent any overlap between the octagonal-shaped annular ring plates. The simulated $|S_{11}|$ at the center frequency was observed to be -18.27 dB, -15.92 dB, -13.75 dB, -11.52 dB, and -9.78 dB (approaching 0 dB) for the different values of

r_3 and r_2 of 9.00 and 8.00 mm; 10.00 and 9.00 mm; 10.00 and 9.00 mm; 11.00 and 10.00 mm; 12.00 and 11.00 mm; and 13.00 mm and 12.00 mm, respectively. Figure 3 (b) depicts the simulation results for the phase of reflection, showing values of -65.98° , -77.10° , -87.94° , -100.42° , and -117.17° (approaching -180.00°) for the pairs r_3 and r_2 of 9.00 and 8.00 mm; 10.00 and 9.00 mm; 10.00 and 9.00 mm; 11.00 and 10.00 mm; 12.00 and 11.00 mm; and 13.00 mm and 12.00 mm, respectively.

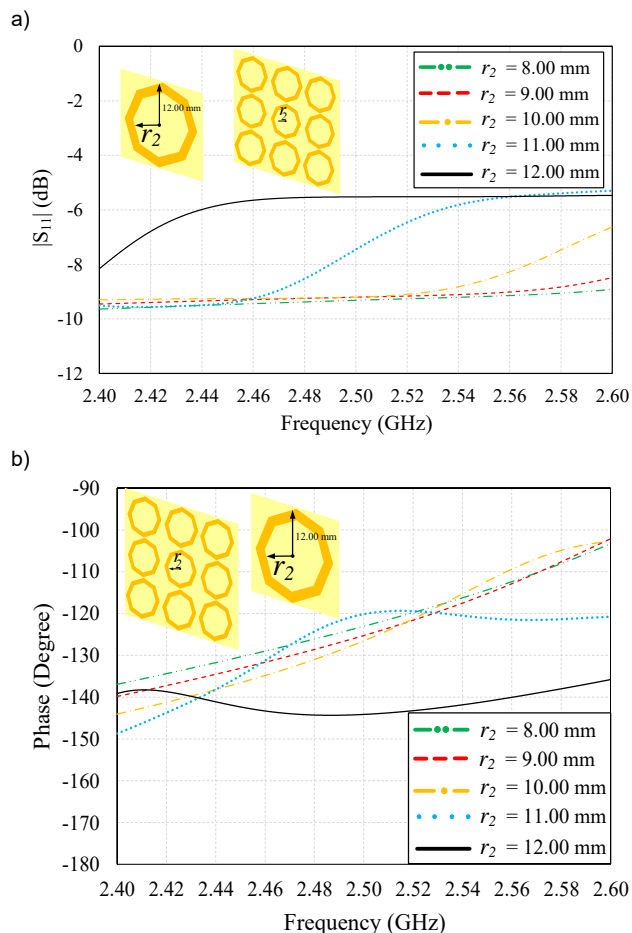


Fig. 4. The simulation results by varying inner radii (r_2) of octagonal-shaped annular ring plate (state#2): a) $|S_{11}|$ and b) phase of the reflection

Figure 4 depicts the inner radii (r_2) of the octagonal-shaped annular ring plate varying from 8.00 to 12.00 mm, respectively, while the outer radii (r_3) of the octagonal-shaped annular ring plate remain fixed at 13.00 mm. The simulated $|S_{11}|$ at the center frequency was obtained of -9.21, -9.20, -9.20, -7.45 and -5.53 dB (approaching 0 dB) for r_2 of 8.00, 9.00, 10.00, 11.00 mm and 12.00 mm, respectively, as shown in Figure 4 (a). Figure 4 (b) illustrates the simulation results also showed that phase of the reflection at the center frequency were occurred -123.03° , -126.24° , -126.57° , -120.07° and 144.13° for r_2 of 8.00 mm, 9.00 mm, 10.00 mm, 11.00 mm and 12.00 mm, respectively. At the central frequency, $|S_{11}|$ was simulated and observed to be -9.21 dB, -9.20 dB, -9.20 dB, -7.45 dB, and -5.53 dB for r_2 radius of 8.00 mm, 9.00 mm, 10.00 mm, 11.00 mm, and 12.00 mm. These results are depicted in Figure 4 (a) as show a trend towards as 0 dB. Figure 4 (b) presents the phase of reflection at the central frequency, with values of -123.03° , -126.24° , -126.57° , -120.07° , and 144.13° for r_2 radius of 8.00 mm, 9.00 mm, 10.00 mm, 11.00 mm, and 12.00 mm, respectively.

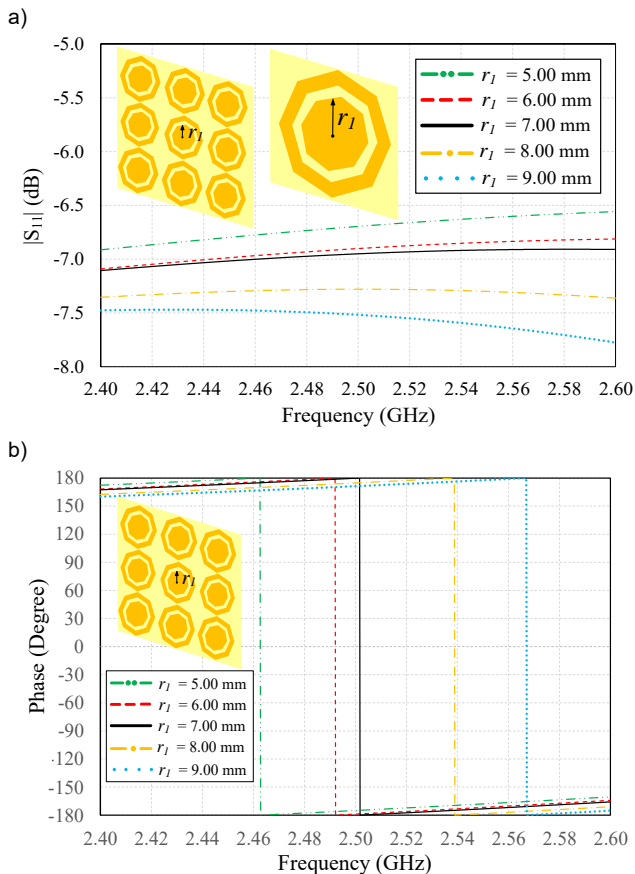


Fig. 5. The simulation results by varying radius (r_1) of octagonal-shaped plate (state#2): a) $|S_{11}|$ and b) phase of the reflection

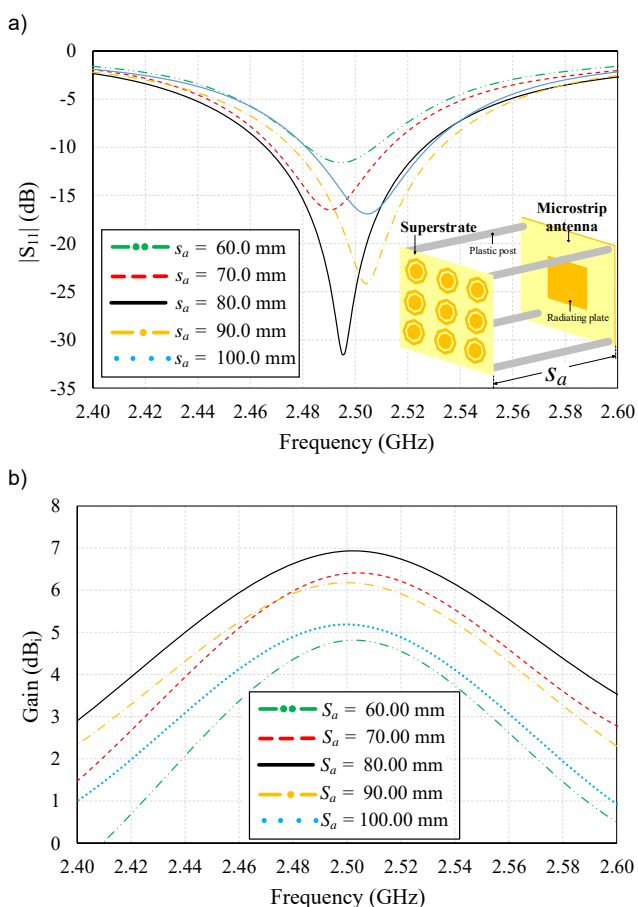


Fig. 6. The simulation results by varied spacing (S_a) of the air gap (state#3): a) $|S_{11}|$ and b) gain

Figure 5 illustrates the variation in the radius (r_1) of the octagonal-shaped plate, ranging from 5.00 mm to 9.00 mm. The values of r_3 and r_2 were fixed at 13.00 mm and 12.00 mm, respectively. The simulated $|S_{11}|$ at the center frequency occurred at -6.69 dB, -6.90 dB, -6.95 dB, -7.28 dB, and -7.52 dB for r_1 values of 5.00 mm, 6.00 mm, 7.00 mm, 8.00 mm, and 9.00 mm, respectively, as depicted in Figure 5 (a). The simulated phase of the reflection at the center frequency is -175.28° , -177.27° , -179.86° , 172.51° and 171.32° for the different values of r_1 as 5.00 mm, 6.00 mm, 7.00 mm, 8.00 mm, and 9.00 mm, respectively. It was found that the r_1 value of 7.00 mm was closest to both -180° and 180° , as shown in Figure 5 (b).

The proposed MS antenna (stage #3), as shown in Figure 1, was integrated between the microstrip antenna (stage #1) and the superstrate layer (stage #2) to enhance radiation gain. Figure 6 illustrates the simulated $|S_{11}|$ and radiation gain for varying air gap spacing (S_a) between the superstrate layer and microstrip antenna, ranging from 60.00 mm to 100.00 mm. In the simulation, it was observed that $|S_{11}|$ and antenna gains are inversely correlated with S_a . Specifically, in Figure 6 (a), the simulated $|S_{11}|$ at the center frequency was measured at -11.24 dB, -14.29 dB, -25.23 dB, -22.18 dB, and -16.52 dB for S_a values of 60.00 mm, 70.00 mm, 80.00 mm, 90.00 mm, and 100.00 mm, respectively. Figure 6 (b) displays the simulated gains at the center frequency, registering values of 4.81 dBi, 6.40 dBi, 6.93 dBi, 6.18 dBi, and 5.19 dBi, respectively.

Simulation and experimental results

This section discusses and compares the simulated results of both the microstrip antenna and the proposed MS antenna, as shown in Figure 7. The comparison reveals a close resemblance between the simulations and the measurements, as depicted in Figures 8–9. The experimented results were measured using an Agilent N5230A network analyzer.

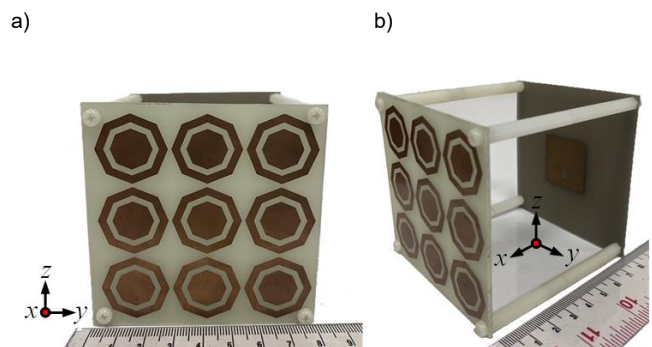


Fig. 7. Photograph of fabricated MS antenna: a) front view and b) cross-sectional views

In Fig. 8 (a), the simulated and measured $|S_{11}|$ values were resonant at a frequency of 2.50 GHz, with $|S_{11}|$ readings of -17.45 dB, -35.79 dB, and -31.55 dB for the microstrip antenna, the MS antenna, and the prototype antenna, respectively. The simulated and measured $|S_{11}|$ bandwidth ($|S_{11}|$ BW) were 2.12% (2.477-2.530 GHz), 2.40% (2.470-2.530 GHz), and 2.40% (2.473-2.533 GHz), respectively. The simulated and measured antenna gains at the center frequency shown in Fig. 8 for the microstrip antenna, the MS antenna, and the prototype antenna were 4.39 dBi, 6.93 dBi, and 6.52 dBi, respectively. Figure 9 and 10 illustrates the simulated and measured radiation patterns of the microstrip, MS and prototype antenna at the center frequency of 2.50 GHz in the x-z plane. The simulated and

measured half-power beamwidths (HPBW) were 79.10°, 54.10°, and 54.60° as shown in Fig.9. Figure 10 depicts the simulated and measured radiation patterns of the microstrip, MS, and prototype antennas at the center frequency of 2.50 GHz in the x-y plane. The simulated and measured half-power beamwidths (HPBW) were 87.10°, 54.8°, and 54.40°, respectively.

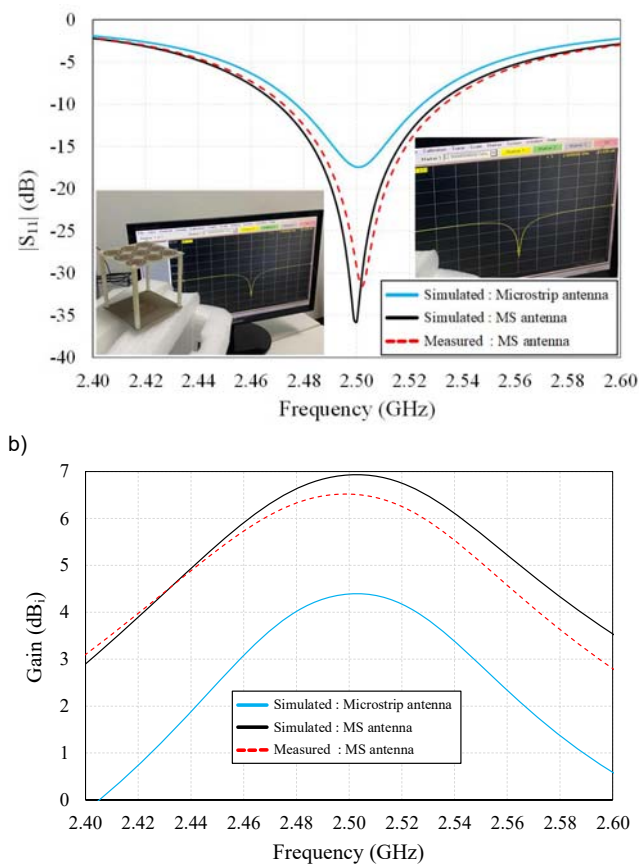


Fig. 8. The simulation and measurement results of the proposed MS antenna: a) $|S_{11}|$ and b) gain

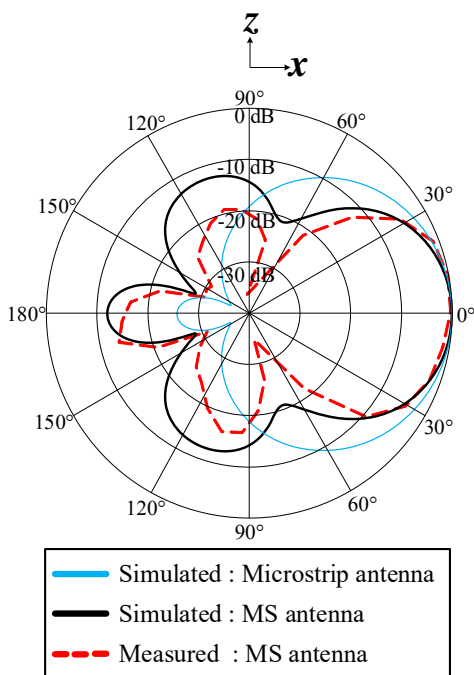


Fig. 9. The simulation and measurement radiation pattern of the proposed MS antenna at 2.5 GHz: in x-z plane

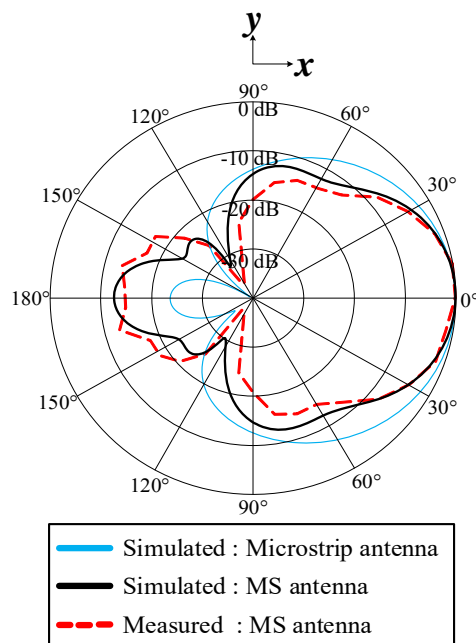


Fig. 10. The simulation and measurement radiation pattern of the proposed MS antenna at 2.5 GHz: in x-y plane

Conclusion

This article provides an overview of the analysis and design of a superstrate layer aimed to enhance the gain of a meta-surface antenna working at a central frequency of 2.50 GHz. Through this scrutiny and design endeavour, which encompassed a superstrate layer comprised of 3x3 unit cells featuring an octagonal-shaped annular ring, it was discovered that the phase of reflection closely approached -179.86° , almost reaching the -180° mark. Operating at 2.50 GHz, the microstrip antenna engineered a unidirectional beam boasting a gain of 4.39 dBi. The integration of the microstrip antenna with the proposed superstrate gave rise to the MS antenna. Positioned a top of an FR4 substrate, the prototype MS antenna achieved a unidirectional beam with a peak gain of 6.93 dBi at the central frequency, representing a surge of over 2.0 dBi in gain. Furthermore, the numerical findings were authenticated through experimental evidence, showcasing an impressive level of consistency. Owing to its elevated radiation gain and favourable radiation characteristics, this proposed antenna emerges as a formidable candidate for integration into modern wireless communication systems, alongside an array of other potential applications.

Acknowledgements

This work has been supported by Funding was also received from the, Thailand Science Research and Innovation (TSRI) and Fundamental Fund of Rajamangala University of Technology Rattanakosin with funding under contract No. FRB6609/2566. The authors acknowledge with gratefulness the resources provided by the Institute of Research and Development (IRD), Rajamangala University of Technology Rattanakosin (RMUTR).

Authors: Komkris Boonying, Department of Telecommunication Engineering, Faculty of Engineering, Rajamangala University of Technology Rattanakosin, Phutthamonthon, Nakhon Pathom, 73170, Thailand, E-mail: komkris.boon@rmutr.ac.th and Ekasit Nugoolcharoenlap, Department of Telecommunication Engineering, Faculty of Engineering, Rajamangala University of Technology Rattanakosin, Phutthamonthon, Nakhon Pathom, 73170, Thailand, E-mail: ekasit.nug@rmutr.ac.th

REFERENCES

- [1] Balanis C. A., *Antenna Theory: Analysis and Design*, Wiley, Hoboken, NJ, 3rd., 2005.
- [2] Bhartia P., Bahl I., Garg R. and Ittipiboon A., *Microstrip Antenna Design Hand book*, Artech House, Inc., 2001.
- [3] Rodney B. W., *Microstrip Patch Antennas: A Designer's Guide*, Springer New York, NY, USA, 2003.
- [4] Arun K., Raghav Kh., Samarth S., Ambuj K. and Arsh M., "A review on gain enhancement techniques of microstrip antenna," *International Conference on Intelligent Engineering and Management (ICIEM)*, pp. 476-479, 2021.
- [5] Wenquan C., Bangning Zh., Aijun L., Tongbin Y., Daosheng G., and Yi W., "Broadband High Gain Periodic Endfire Antenna by Using I-Shaped Resonator (ISR) Structures," *IEEE Antennas and Wireless Propagation Letters*, vol. 11, pp. 1470-1473, 2012.
- [6] Hao W., Shu -F. L., Lei Ch., Wen -T. L. and Xiao -W. Sh. "Gain Enhancement for broadband Vertical Planar Printed Antenna With H-Shaped Resonator Structures," *IEEE Transactions on Antennas and Propagation*, vol. 62, issue 8, pp. 4411-4415, 2014.
- [7] Amit K. S., Mahesh P. Ab. and Shiban K. K., "High-gain and High-Aperture-Efficiency cavity resonator antenna using metamaterial superstrate," *IEEE Antennas and Wireless Propagation Letters*, vol. 16, pp. 2388-2391, 2017.
- [8] Khoutar F.Z., Aznabet M., Mrabet O. EL., "Gain and Directivity Enhancement of a Rectangular Microstrip Patch Antenna using a Single Layer Metamaterial Superstrate," *International Conference on Multimedia Computing and System (ICMCS)*, 2018
- [9] Muftah A., Islam A. and Abdel -R. S., "High Gain and Wideband High Dense Dielectric Patch Antenna Using FSS Superstrate for Millimeter-Wave Applications," *IEEE Access*, vol.6, pp. 38243-38250, 2018.
- [10] Kim J. H., Ahn C. and Bang J., "Antenna Gain Enhancement Using a Holey Superstrate," *IEEE Transactions on Antennas and Propagation*, vol. 64, no. 3, pp. 1164-1167, 2016.
- [11] Asaadi M. and Sebak A. "Gain and Bandwidth Enhancement of 2x2 Square Dense Dielectric Patch Antenna Array Using a Holey Superstrate," *IEEE Antennas and Wireless Propagation Letters*, vol. 16, pp. 1808-1811, 2017.
- [12] Jinhai L., Zhaoyang T., Ziyang W., Hui L. and Yingzeng Y., "Gain Enhancement of a Broadband Symmetrical Dual-Loop Antenna Using Shorting Pins," *IEEE Antennas and Wireless Propagation Letters*, vol. 17, issue 8, pp. 1369-1372, 2018.
- [13] Arun K., Santanu Dw. And Ganga P. P., "A dual-band high-gain microstrip antenna with a defective frequency selective surface for wireless applications," *Journal of Electromagnetic Waves and Applications*, Taylor & Francis, pp. 1-14, 2021
- [14] Pooja P., Mahesh P. Ab., Ananjan B. and Shiban K. K., "Gain enhancement of a CPW-fed monopole antenna using polarization insensitive AMC structure," *IEEE Antennas and Wireless Propagation Letters*, vol. 12, pp. 1315-1318, 2013.
- [15] Siew B. Y. and Zhi N. Ch. "Microstrip Patch Antennas with Enhanced Gain by Partial Substrate Removal," *IEEE Transactions on Antennas and Propagation*, vol. 58, no, 9, pp. 2811-2816, 2010.
- [16] Kingsta R. M. and Seyatha K., "Design and Performance Comparison of Metamaterial Superstrate Antenna for DSRC Applications," *International Conference on Trends in Electronics and Informatics (ICOEI)*, 2019.
- [17] Aqeel H. N. and Sungjoon L., "A Beam-Steering Antenna with a Fluidically Programmable Metasurface," *IEEE Transactions on antennas and propagation*, vol. 67, no. 6, pp. 3704-3711, 2019.
- [18] Diptiranjana S. and Somak Bh., "A Gain-Enhanced Slotted Patch Antenna Using Metasurface as Superstrate Configuration," *IEEE Transactions on antennas and propagation*, vol. 68, no. 9, pp. 6548-6556, 2020.
- [19] Chandrashekar K. S., Halappa G., Koushik D., Poomima S. and Chandramma S., "A Wideband Design of Microstrip Patch Antenna Loaded with Metal Ring Superstrate," *IEEE Indian Conference on Antennas and Propagation (InCAP)*, 2020.
- [20] Avanish Y. Ashwani K. and Prashant Ch., "High Gain Wideband Antenna using Metasurface Horn and Metasurface Superstrate," URSI Regional Conference on Radio, 2020.
- [21] Luiza L., Mateusz R., Krzysztof N. and Lukasz, "High-Gain Compact Circularly Polarized X-Band Superstrate Antenna for CubeSat Applications," *IEEE Antennas and Wireless Propagation Letters*, vol. 20, no. 11, 2090-2094, 2021.
- [22] Tamara Z. F., Noor A. M., Mohamad K. A. R., Hamid M. R. and Levy O. N., "A Beam-Spilt Metasurface Antenna for 5G Applications," *IEEE Access*, vol. 10, pp. 1162-1174, 2022.
- [23] Anirban Ch., Koushik, Satyajit Ch. And Raj M., "Advance Design of High-Gain Fabry-Perot Cavity Antenna Offering Wide Common Impedance and Gain Bandwidth," *IEEE antennas and wireless propagation letters*, vol. 22, no. 5, pp. 1214-1218, 2023.
- [24] CST® Microwave Studio, Research Base, 2020.